

# **Dangerous liaisons between detergents and membrane proteins. The case of mitochondrial uncoupling protein 2.**

Manuela Zoonens<sup>1,2</sup>, Jeffrey Comer<sup>3,4</sup>, Sandrine Masscheleyn<sup>1,2</sup>, Eva Pebay-Peyroula<sup>5,6,7</sup>,  
Christophe Chipot<sup>3,4,8</sup>, Bruno Miroux<sup>1,2\*</sup> and François Dehez<sup>3,4,8\*</sup>

## **Supplementary Information**

### **Affiliations**

<sup>1</sup> CNRS UMR 7099, Institut de Biologie Physico Chimique (IBPC), 75005 Paris, France.

<sup>2</sup> Université Paris-Diderot, IBPC, 75005 Paris, France.

<sup>3</sup> CNRS UMR 7565, Structure et Réactivité des Systèmes Moléculaires Complexes (SRSMC),  
54500 Vandoeuvre-les-Nancy, France.

<sup>4</sup> Université de Lorraine, SRSMC, 54500 Vandoeuvre-les-Nancy, France.

<sup>5</sup> Univ. Grenoble Alpes, Institut de Biologie Structurale (IBS), F-38027 Grenoble, France .

<sup>6</sup> CEA, DSV, IBS, F-38027 Grenoble, France.

<sup>7</sup> CNRS, IBS, F-38027 Grenoble, France.

<sup>8</sup> Laboratoire International Associé CNRS and University of Illinois at Urbana-Champaign,  
54506 Vandoeuvre-lès-Nancy.

### **\* Corresponding authors**

Bruno Miroux, tel: +33 (0)1 5841 5225 ; email: bruno.miroux@ibpc.fr

François Dehez, tel: +33 (0)3 8368 4098 ; email: Francois.Dehez@univ-lorraine.fr

## Supplementary Methods

### *Molecular representations*

For all molecular representations, the protein backbone was aligned consistently onto the same reference structure (pdb:2LCK). The cross-sections were made systematically along the same longitudinal plane containing the central axis of the protein.

### *UCP2 in DPC*

Extensive sampling of DPC/UCP2 interactions was made through a series of all-atom and coarse-grain simulations. The self-assembly of DPC around UCP2 was first simulated by all-atom MD simulations of 100 ns at detergent:protein ratios of 120, 240 and 600 respectively. Starting from random monodisperse solutions of DPC at 200  $\mu\text{M}$ , MD simulations were carried out with NAMD following the same protocol and using the same force field described in the manuscript Methods section. We next performed a series of 1  $\mu\text{s}$  coarse-grain simulations to obtain a statistical description of DPC organization around UCP2. Three detergent:protein ratios of 200, 250 and 300 were considered with a 200  $\mu\text{M}$  concentration DPC. For each system, eight initial configurations were generated by randomly positioning DPC around UCP2 in its NMR structure (pdb:2LCK). MD simulations were carried out with NAMD<sup>1</sup>. The coarse-grain particles were described by the MARTINI2<sup>2</sup> force field. Equations of motion were integrated with a time step of 30 fs. Non-bonded interactions were truncated at a spherical cutoff distance of 12 Å. All trajectories were generated in the NPT isobaric-isothermal ensemble, at 310 K under 1 atm using, respectively, Langevin dynamics<sup>3</sup> (damping coefficient, 1  $\text{ps}^{-1}$ ) and the Langevin piston method<sup>4</sup>. For all trajectories, UCP2 coarse-grain particles were constrained to their initial position. As in the in all-atom simulations, the formation of a bundle of DPC around the hydrophobic core of UCP2 was systematically observed and DPC molecules self-assembled into micelles on both the matrix and the

cytoplasmic sides of the protein, catalyzed by two amphiphilic segments exposed to the solvent: residues 29 to 59 and 298 to 308 respectively.

Starting from the end-point structure of the all-atom MD with 600 DPC, we superimposed all final MD configurations and build a model in which all observed steadily DPC-UCP2 interactions were included, except when steric clashes preventing added some DPC molecules. The resulting structure involved 300 DPC molecules distributed all over the surface and within the cavity UCP2.

#### *Effective radii of proteins internal cavity*

We sought to characterize the size of the water channel through the UCP2 protein in a way that would permit comparison among the structures analyzed in this work as well as comparisons to other membrane proteins. However, the complex topology of the channel through the UCP2 NMR structure made difficult the application of algorithms that assume a pore of cylindrical symmetry, for example that employed by Aksimentiev and Schulten<sup>5</sup>. Therefore, we developed an algorithm that produced results similar to those of the Aksimentiev and Schulten algorithm for approximately cylindrical channels, while also being applicable to the more complex internal structures analyzed in this work.

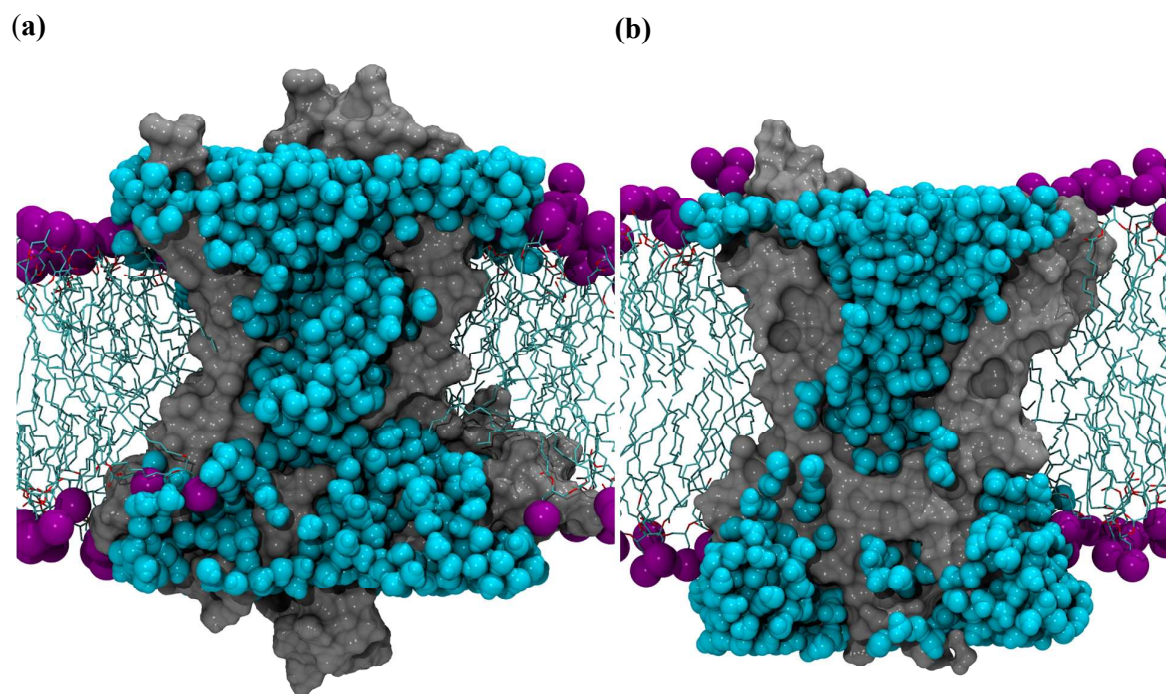
First, we extracted 10 frames at 1 ns intervals from the final 10 ns of each MD simulation. We analyzed the simulations of unconstrained UCP2-GDP<sup>3-</sup> in a POPC membrane, unconstrained UCP2-GDP<sup>3-</sup> embedded in DPC micelles, and UCP2-GDP<sup>3-</sup> in a POPC membrane with the backbone atoms constrained to their positions in pdb:2LCK. For comparison, we also analyzed a simulation of unconstrained AAC in a POPC membrane. In the simulations in which the UCP2 or AAC backbone was unconstrained, the frames were taken from the interval 165–175 ns. To facilitate comparison, we applied the rigid transformation that minimized the root-mean-squared deviation of the C atoms from their positions in pdb:2LCK.

For AAC, another reference structure was used. In the description of the algorithm below, the  $z$ -axis was defined to be perpendicular to the membrane.

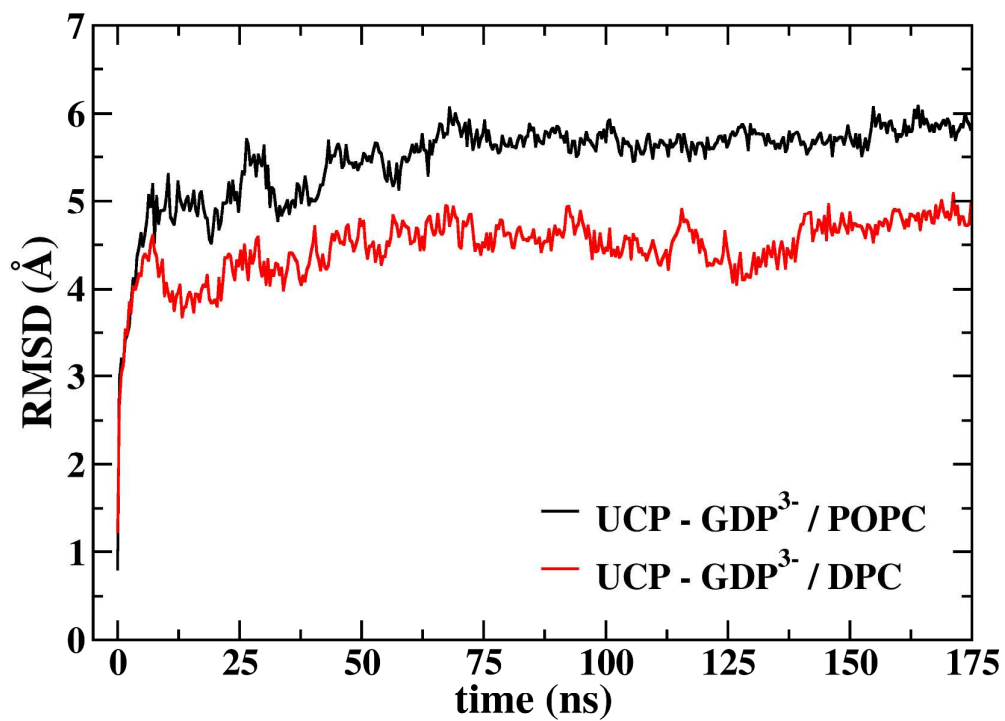
The excluded space of the protein in each trajectory frame was represented on a 0.3 Å-resolution cubic grid and was defined as including all grid nodes less than  $R_{\min}/2 + 0.5$  Å from the center of any atom, where  $R_{\min}/2$  was the Lennard-Jones size parameter for the atom in question taken from the CHARMM force field<sup>6</sup>. The extra 0.5 Å was added to prevent small water inaccessible cavities that appear in the instantaneous structure from being included as part of the channel.

To define the empty space within the protein, an algorithmic definition of the "within the protein" was needed. For each node of the grid not within the excluded space of the protein, we generated 400 lines in  $xy$  plane with random directions emanating from the node. Nodes were considered to be within the protein when a majority of these lines intersected the excluded space of the protein in both directions from the node. Contiguous regions were defined by nodes of empty space within the protein whose nearest neighbors were also nodes of empty space within the protein. The channel domain was then defined as the largest contiguous region of empty space within the protein. The cross sectional area of the channel domain at each value of  $z$  was averaged over the ten frames of each simulation. Finally, the effective radius of the channel was calculated as  $r_{\text{eff}} = (A(z)/\pi)^{1/2}$ .

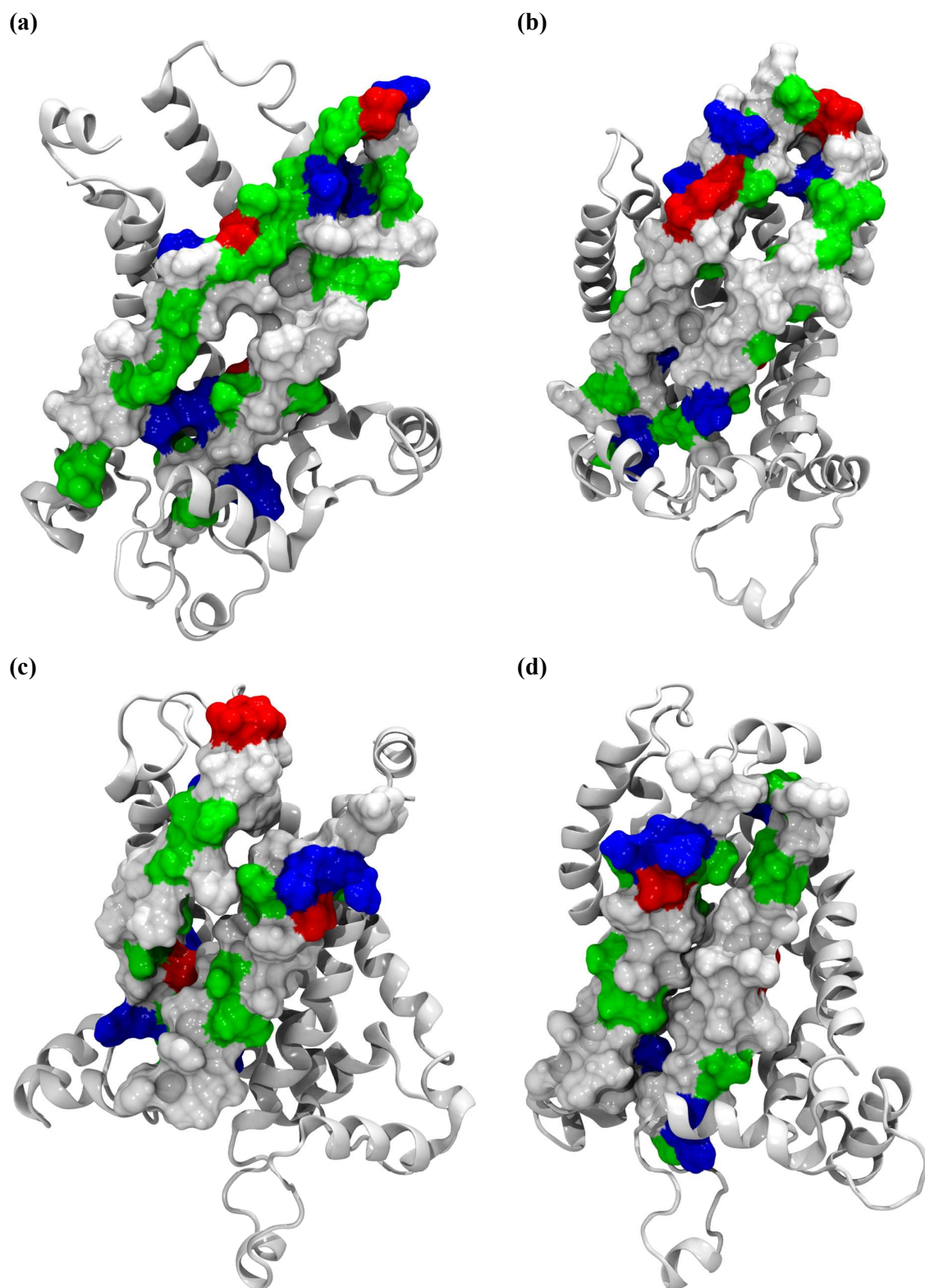
## Supplementary Figures



**Supplementary Figure S1: The UCP2 NMR structure acts as a large transmembrane channel** (A) Cross-sectional view of UCP2-*apo* embedded in a POPC bilayer. Backbone atoms are constrained to their original positions in pdb:2LCK. A large water channel, spanning the entire protein, connects the two sides of the membrane. (B) Cross-sectional view of AAC-*apo* embedded in a POPC bilayer (Dehez et al. 2008). The protein is fully occluded on the matrix side and prevents water to cross the bilayer. The protein surface is colored in grey. Violet and cyan spheres represent phospholipid headgroups and water molecules, respectively. Phosphorus, nitrogen, oxygen and carbon atoms of nucleotides are colored in brown, blue, red and green, respectively.

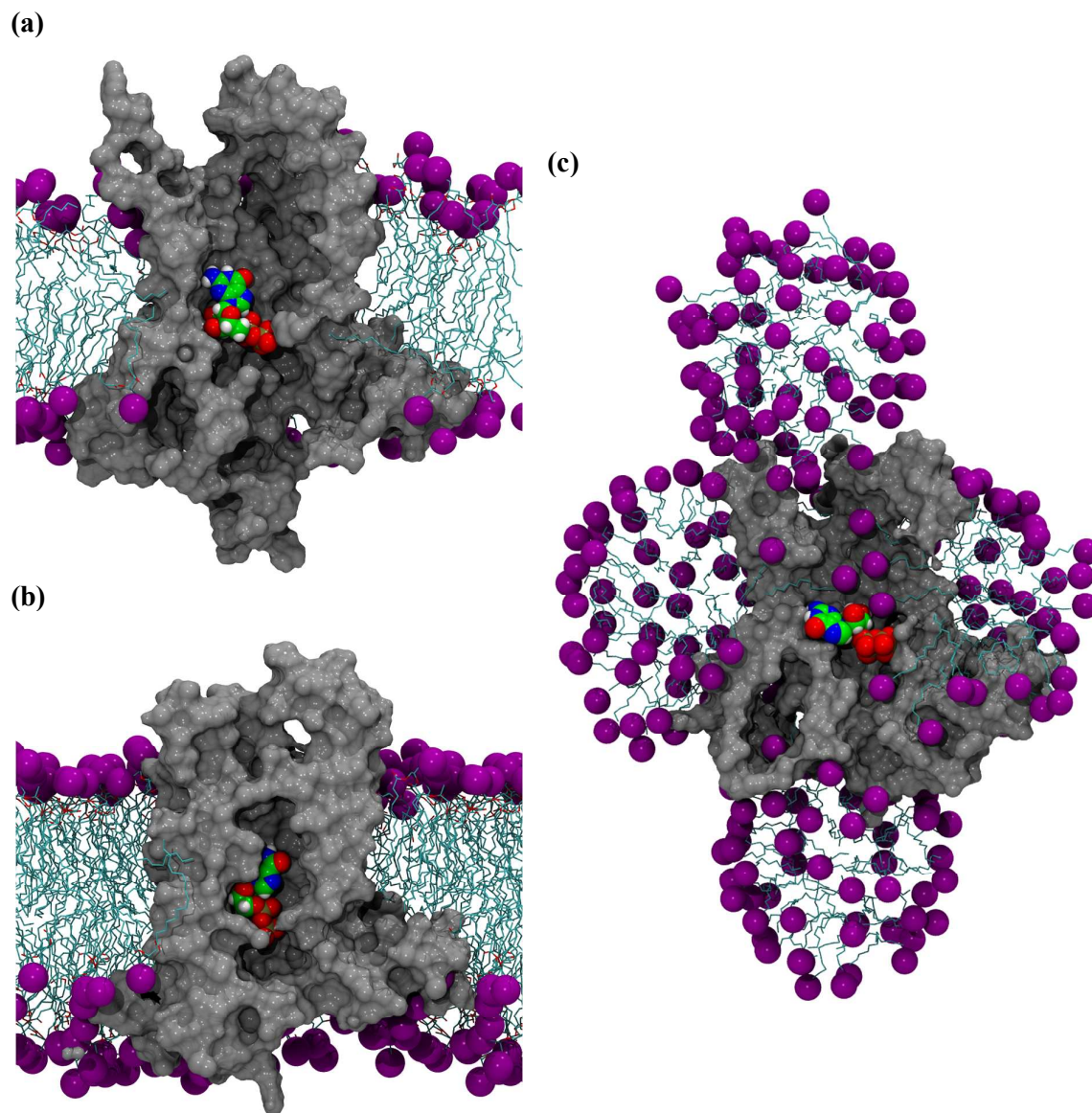


**Supplementary Figure S2: Evolution of backbone positional root-mean-square-deviation** from the 2LCK NMR of UCP2 in complex with GDP<sup>3-</sup> in (black) POPC and (red) DPC.



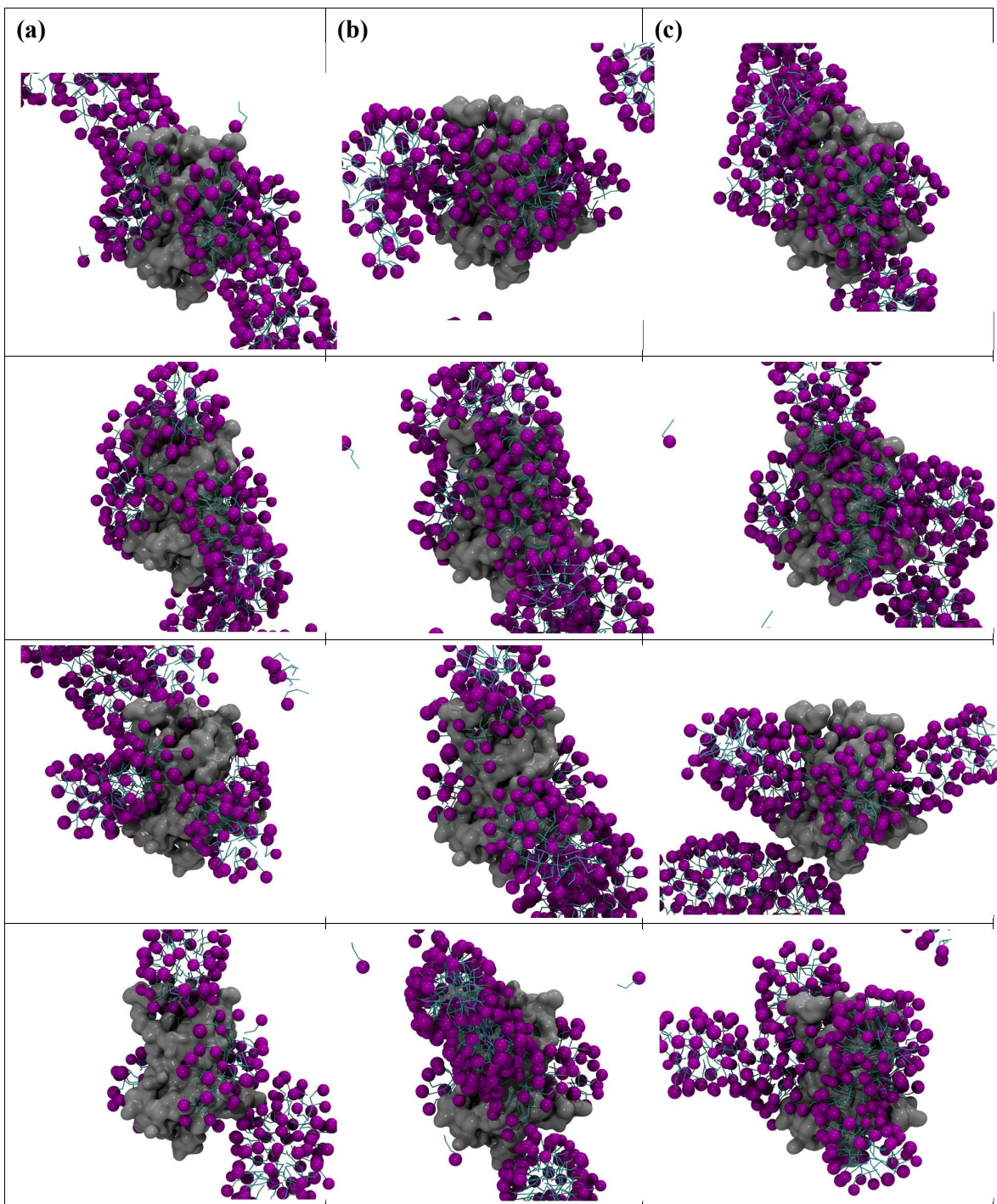
**Supplementary Figure S3: Molecular views of the interstitial spaces between helices in PDB structure 2LCK. (a) Helices H2-H3. (b) Helices H4-H5. (c) Helices H5-H6. (d) Helices**

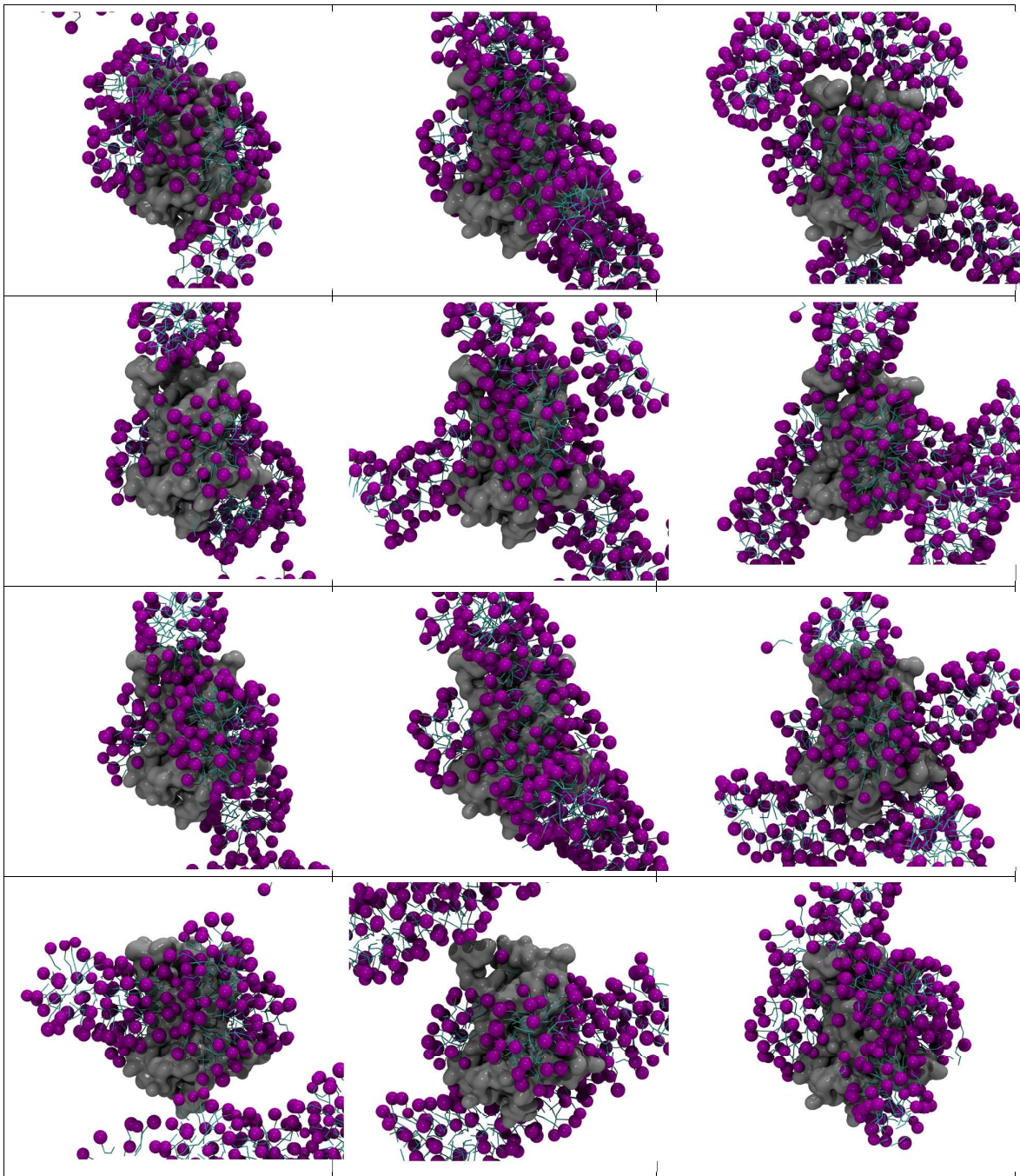
H6-H1. Hydrophobic, polar, acidic and basic residues are depicted as white, green, red and blue surface patches, respectively.



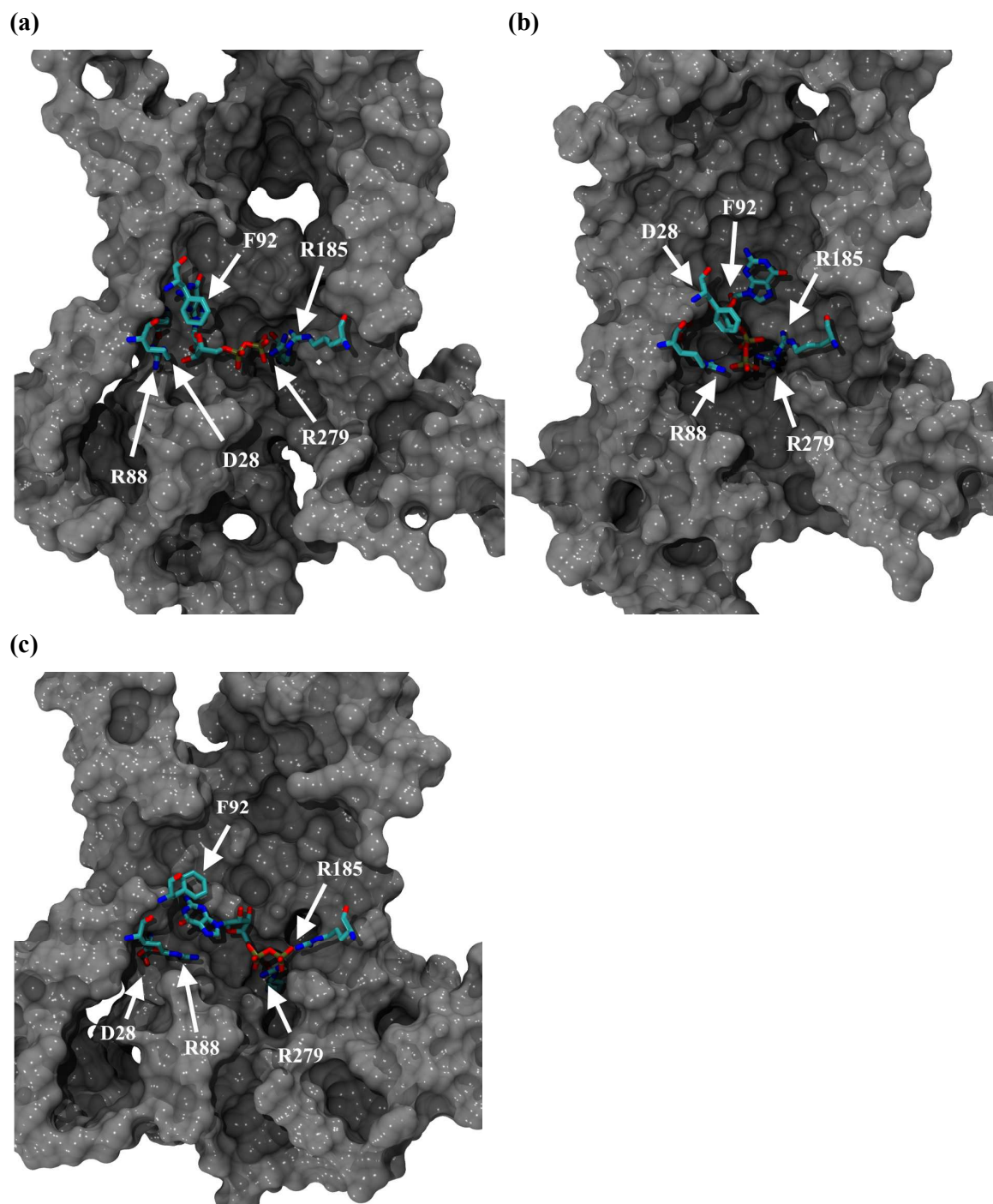
**Supplementary Figure S4:** (a) Cross-sectional view of UCP2-GDP<sup>3-</sup> embedded in a POPC bilayer. Backbone atoms are constrained to their reference positions from PDB structure 2LCK. (b) Cross-sectional view of UCP2-GDP<sup>3-</sup> embedded in a POPC bilayer after full relaxation of the entire protein. (d) Cross-sectional view of UCP2-GDP<sup>3-</sup> embedded in DPC micelles after full relaxation of the entire protein. Detergent molecules are organized in a

bundle around the hydrophobic core of the protein. Two extra micelles form on the matrix and cytoplasmic sides around amphiphilic patches of amino acids. The internal cavity of the protein is fully opened, in a conformation akin to that observed in the backbone-constrained simulation. Violet spheres represent phospholipid head groups. Phosphorus, nitrogen, oxygen and carbon of nucleotides are colored in brown, blue, red and green, respectively.

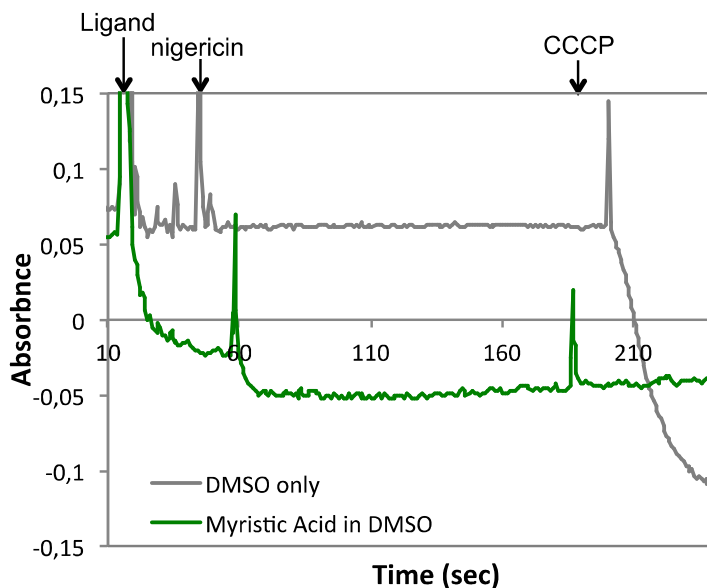




**Supplementary Figure S5: Self-assembly of DPC around UCP2.** Final configurations of eight independent, 1- $\mu$ s coarse-grained simulations carried out at 200  $\mu$ M of DPC and with a detergent:protein ratio of (a) 200, (b) 250 and (c) 300, consistent with experimental conditions. A bundle of DPC systematically forms around the hydrophobic core of the protein. In addition, segments exposed to the solvent on the cytoplasm (residue 298 to 308) and matrix (residue 29 to 59) sides catalyze the formation of extra DPC micelles.



**Supplementary Figure S6: Close view of the putative binding site of GDP<sup>3-</sup> involving D28, R88, F92, R185 and R279 in (a) POPC with UCP2 backbone constrained, (b) POPC with no positional restraints and (c) DPC with no positional restraints.**



**Supplementary Figure S7: Effect of myristic acid on liposomes.** Liposomes (without any protein incorporated in) show a strong conductance upon addition of 1 mM myristic acid (dissolved in DMSO) even before the addition of nigericin. A control experiment was performed with the same volume of DMSO. At the end of the kinetics, CCCP was added to check the liposome integrity.

## REFERENCES

1. Phillips, J. C. *et al.* Scalable molecular dynamics with NAMD. *J. Comp. Chem.* **26**, 1781–1802 (2005).
2. De Jong, D. H. *et al.* Improved Parameters for the Martini Coarse-Grained Protein Force Field. *J. Chem. Theo. Comp.* **9**, 687–697 (2013).
3. Feller, S. E., Zhang, Y., Pastor, R. W. & Brooks, B. R. Constant pressure molecular dynamics simulation: The Langevin piston method. *J. Chem. Phys.* **103**, 4613 (1995).
4. Martyna, G. J., Tobias, D. J. & Klein, M. L. Constant pressure molecular dynamics algorithms. *J. Chem. Phys.* **101**, 4177 (1994).

5. Aksimentiev, A. & Schulten, K. Imaging  $\alpha$ -Hemolysin with Molecular Dynamics: Ionic Conductance, Osmotic Permeability, and the Electrostatic Potential Map. *Biophys. J.* **88**, 3745–3761 (2005).
6. MacKerell, A. D. *et al.* All-Atom Empirical Potential for Molecular Modeling and Dynamics Studies of Proteins. *J. Phys. Chem. B* **102**, 3586–3616 (1998).